The British University in Egypt

BUE Scholar

Basic Science Engineering

Engineering

2019

A finite element solution of Bergan-Wang plate model

Kamal Hassan Prof.
Department of Basic Science, Faculty of Engineering, The British University in Egypt, kamal.hassan@bue.edu.eg

Ehab Ali
Academy of Science, Cairo, Egypt, mohammad.tawfik@gmail.com

Ehab Ali
Department of Basic Science, Faculty of Engineering, Banha University, eng.ehabmagdy@gmail.com

Recommended Citation

PAPER • OPEN ACCESS

A finite element solution of Bergan-Wang plate model

View the article online for updates and enhancements.

A finite element solution of Bergan-Wang plate model

Kamal Hassan[1], Ehab Ali[2] and Mohammad Tawfik[3]

[1]Department of basic science, the British University in Egypt, Cairo, Egypt
[2]Department of basic science, Banha University, Banha, Egypt
[3]Academy of Knowledge, Cairo, Egypt

Email:

Abstract. Bergan-Wang approach has led to a formulation of the strain energy of a plate bending deflection as function of only the transversal deflection of the plate. In this paper, two rectangular plate bending finite elements are introduced, using new degrees of freedom based on Bergan-Wang approach for analysis of thin, moderately thick plates, in terms of this unique variable. The first element has four nodes with 24 DOF while the second has 36 DOF. These two elements are conforming in case of thin plates. Adopting the usual 3 boundary conditions of Reissner-Mindlin theory, variety of examples have been analysed for thin and moderately thick plate bending problems with plurality of finite element meshes and a variety of thickness to plate length ratios with different boundary conditions on sides. As typical characteristics of Bergan-Wang approach, there is no locking as the thickness decreases and convergence to the classical thin plate solution is achieved. Comparison with Reissner-Mindlin and 3D solutions supports the study.

1. Introduction

The analysis of thin and thick plate bending with different types of boundary conditions is a main common problem in many engineering fields, such as concrete pavements, aerospace, and structural and mechanical engineering [1].

Commercial finite element codes which are used for the analysis of plate bending are usually based on Reissner - Mindlin theory. This theory incorporates the effects of transverse shear deformation and its strain energy expression involves three independent variables: the lateral deflection w and the two plate rotations ϕ_x , ϕ_y [2, 3].

On the other hand, Bergan-Wang assumptions have led to a strain energy expression using only one variable which is the lateral deflection w. This has been achieved by expressing the shear rotations as functions of the third derivatives of deflection. As a result of this their assumptions, the lower the thickness of the plate the closer the strain energy expressions to the expressions of the classical thin plate theory. This occurs without suffering from the locking phenomena known in finite element application [4].

A new non-conforming quadrilateral finite element for thin and thick plates is described by Bergan and Wang [5]. This element is based on a "free formulation" which checks convergence and appropriate rank of stiffness. It is formulated in a way that allows for selection of element displacement modes without the need to consider the compatibility between the elements. And therefore, Shear deformations can be easily incorporated according to Reissner - Mindlin plate theory. It should be noted that the usual

approach of expressing transverse displacements and rotations by separate expansions is not followed [5].

2. Analysis of Bergan – Wang approach

The Reissner-Mindlin hypothesis of plate bending theory is that the perpendicular line to the middle plane of the un-deformed plate remains straight, but not must be perpendicular to the deformed mid-surface (figure 1)
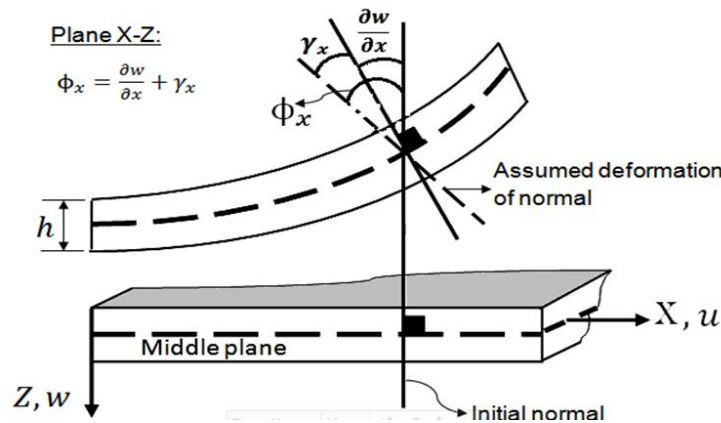
Figure 1. Middle plane of the plate and normal line before and after deformation

Accordingly, the displacement field of this theory is as follow [6]:

$$u(x, y, z) = -z\,\phi_x(x, y)$$
$$v(x, y, z) = -z\,\phi_y(x, y) \tag{1}$$
$$w(x, y, z) = w(x, y)$$

where, w is the lateral deflection in z-direction, ϕ_x and ϕ_y are the rotation of normal vector about x-axis and y-axis respectively.

$$\phi_x = \frac{\partial w}{\partial x} + \gamma_x \quad ; \quad \phi_y = \frac{\partial w}{\partial y} + \gamma_y \tag{2}$$

where, γ_x and γ_y resulting from the lack of orthogonality of the perpendicular line to the middle plane after deformation.

The linear strains related with this displacement field can be written:

$$\epsilon = \left\{ \begin{matrix} \epsilon_b \\ \cdots\cdots \\ \epsilon_s \end{matrix} \right\} = \left\{ \begin{matrix} \epsilon_x \\ \epsilon_y \\ \epsilon_{xy} \\ \cdots\cdots \\ \gamma_x \\ \gamma_y \end{matrix} \right\} = \left\{ \begin{matrix} -z\dfrac{\partial \phi_x}{\partial x} \\ -z\dfrac{\partial \phi_y}{\partial y} \\ -z\left(\dfrac{\partial \phi_x}{\partial y} + \dfrac{\partial \phi_y}{\partial x}\right) \\ \cdots\cdots\cdots\cdots\cdots\cdots \\ \phi_x - \dfrac{\partial w}{\partial x} \\ \phi_y - \dfrac{\partial w}{\partial y} \end{matrix} \right\} \tag{3}$$

The stresses across the thickness (h) can be recovered from the generalized strains Eq. (3) as

$$\sigma = \left\{ \begin{matrix} \sigma_b \\ \cdots \\ \sigma_s \end{matrix} \right\} = \begin{bmatrix} D_b & \vdots & 0 \\ \cdots & \vdots & \cdots \\ 0 & \vdots & D_s \end{bmatrix} \left\{ \begin{matrix} \epsilon_b \\ \cdots \\ \epsilon_s \end{matrix} \right\} \tag{4}$$

where, D_b and D_s are the matrices of flexural and shear rigidities for an isotropic and homogeneous elastic plate.

$$D_b = \frac{E\,h^3}{12(1-v^2)} \begin{bmatrix} 1 & v & 0 \\ v & 1 & 0 \\ 0 & 0 & (1-v)/2 \end{bmatrix} \quad ; \quad D_s = \frac{kE\,h}{2(1+v)} \begin{bmatrix} 1 & 0 \\ 0 & 1 \end{bmatrix} \tag{5}$$

where, k is the shear modification factor and is normally set equal to 5/6 for isotropic homogeneous plates.

Bending moments, twisting moments and vertical shear forces per unit length can be obtained by integrating the stresses distributed over the thickness of the plate [7].

$$\left\{ \begin{matrix} M_x \\ M_y \\ M_{xy} \\ \cdots \\ Q_x \\ Q_y \end{matrix} \right\} = \int_{-\frac{h}{2}}^{\frac{h}{2}} \left\{ \begin{matrix} -z\sigma_b \\ \cdots \\ \sigma_s \end{matrix} \right\} dz \tag{6}$$

Assuming a positive lateral force P acting on an infinitesimal plate bending element $dxdy$ (figure. 2),
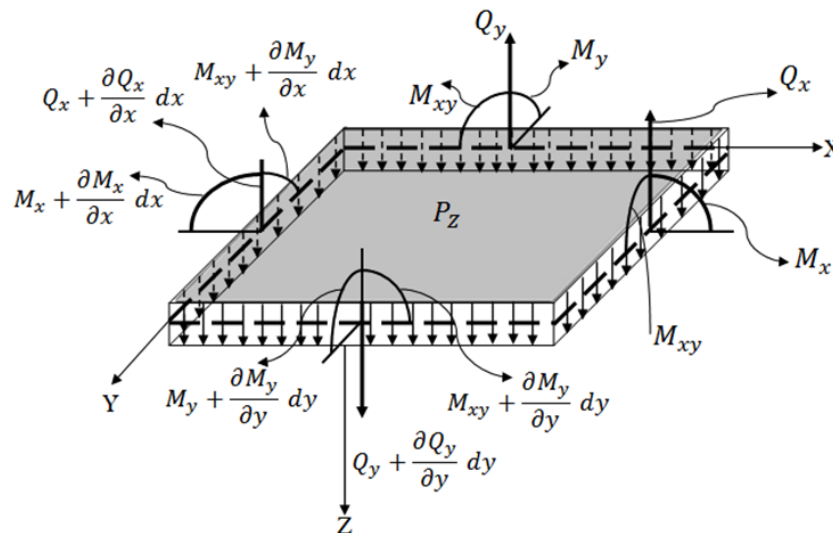
Figure 2. Moments, loads and shear forces in an infinitesimal plate element

By applying the equilibrium conditions on the plate element, it is of interest to note the relations between the two shearing forces, Q_x and Q_y, two moments, M_x and M_y and twisting moment, M_{xy} are obtained as [8].

$$Q_x = M_x - M_{xy}$$

$$Q_y = M_y - M_{xy} \qquad (7)$$

It is possible to infer a relationship between the shear strains and the transverse displacement by substituting with strain field (3) and the constitutive relations (4) and (6) in the equilibrium equations (7).

$$\gamma_x = \frac{h^2}{5(1-v)}\left[\frac{\partial^3 w}{\partial x^3} + \frac{\partial^3 w}{\partial x \partial y^2} + \frac{\partial^2 \gamma_x}{\partial x^2} + \frac{(1-v)}{2}\frac{\partial^2 \gamma_x}{\partial y^2} + \frac{(1+v)}{2}\frac{\partial^2 \gamma_y}{\partial x \partial y}\right]$$

$$\gamma_y = \frac{h^2}{5(1-v)}\left[\frac{\partial^3 w}{\partial y^3} + \frac{\partial^3 w}{\partial y \partial x^2} + \frac{\partial^2 \gamma_y}{\partial y^2} + \frac{(1-v)}{2}\frac{\partial^2 \gamma_y}{\partial x^2} + \frac{(1+v)}{2}\frac{\partial^2 \gamma_x}{\partial x \partial y}\right] \qquad (8)$$

Bergan − Wang approach assumes that the shear deformations for a limited area of the plate are dominated by a constant term, or, at most, in part also by a linear term [5].

The meaning of this assumption can be understood as an approximation of the integral representing the strain energy. This, from one side is be very suitable for finite element solution, and from another side keeps the same boundary conditions as defined according to Reissner-Mindlin theory.

Therefore, the shear strains are given by:

$$\gamma_x \cong h_0{}^2\left[\frac{\partial^3 w}{\partial x^3} + \frac{\partial^3 w}{\partial x \partial y^2}\right] \quad ; \quad \gamma_y \cong h_0{}^2\left[\frac{\partial^3 w}{\partial y^3} + \frac{\partial^3 w}{\partial y \partial x^2}\right] \qquad (9)$$

where

$$h_0{}^2 = \frac{h^2}{5(1-v)} \qquad (10)$$

And based on relation (9), the rotation of the normal vector (2) can be expressed in terms of the lateral deflection as:

$$\phi_x = w_{,x} + h_0^2\left[w_{,xxx} + w_{,xyy}\right]$$

$$\phi_y = w_{,y} + h_0^2\left[w_{,yyy} + w_{,yxx}\right] \qquad (11)$$

This in turn can be replaced in the strain field (3) as

$$\epsilon_b = \begin{bmatrix} w_{,xx} + h_0^2\left(w_{,xxxx} + w_{,xxyy}\right) \\ w_{,yy} + h_0^2\left(w_{,yyyy} + w_{,xxyy}\right) \\ 2w_{,xy} + 2h_0^2\left(w_{,xyyy} + w_{,xxxy}\right) \end{bmatrix} \quad ; \quad \epsilon_s = h_0^2\begin{bmatrix} \left(w_{,xxx} + w_{,xyy}\right) \\ \left(w_{,yyy} + w_{,xxy}\right) \end{bmatrix} \qquad (12)$$

Based on the relations of (12), the strain energy of Bergan-Wang approach is expressed as function of one variable: the lateral deflection $w(x, y)$.

3. The finite element formulations of the two elements

Two new finite elements are proposed. Based on the existing finite elements, new degrees of freedoms are adopted keeping the same shapes (rectangles) and the same polynomial (complete polynomial of degree four for the first element and five for the other one plus additional monomes).

3.1. The first finite element which will be denoted BWRE24

The displacement field is introduced at each node (i) as:

$$\{w\}_i^T = \{w|\phi_x|\phi_y|\epsilon_x|\epsilon_y|\epsilon_{xy}\}_i \tag{13}$$

By using the new expressions based on Bergan – Wang approach in (3), (11), (12), the result of the six nodal variables (degrees-of-freedom) at each node is a 24-degree of freedom element. Therefore the deflection can be expressed as [9].

$$
\begin{aligned}
w(x,y) = {} & \boldsymbol{\alpha_1} + \boldsymbol{\alpha_2}x + \boldsymbol{\alpha_3}y + \boldsymbol{\alpha_4}x^2 + \boldsymbol{\alpha_5}xy + \boldsymbol{\alpha_6}y^2 + \boldsymbol{\alpha_7}x^3 + \boldsymbol{\alpha_8}x^2y + \boldsymbol{\alpha_9}xy^2 \\
& + \boldsymbol{\alpha_{10}}y^3 + \boldsymbol{\alpha_{11}}x^4 + \boldsymbol{\alpha_{12}}x^3y + \boldsymbol{\alpha_{13}}x^2y^2 + \boldsymbol{\alpha_{14}}xy^3 + \boldsymbol{\alpha_{15}}y^4 + \alpha_{16}x^5 \\
& + \alpha_{17}x^2y^3 + \alpha_{18}x^3y^2 + \alpha_{19}y^5 + \alpha_{20}x^4\left(\frac{1}{2}yb - \frac{2}{3}\frac{y^3}{b}\right) \\
& + \alpha_{21}y^4\left(\frac{1}{2}xa - \frac{2}{3}\frac{x^3}{a}\right) + \alpha_{22}x^3y^3 + \alpha_{23}x^5\left(\frac{1}{2}yb - \frac{2}{3}\frac{y^3}{b}\right) \\
& + \alpha_{24}y^5(\frac{1}{2}xa - \frac{2}{3}x^3/a)
\end{aligned}
\tag{14}
$$

where, a and b are the dimensions of the rectangular plate element.
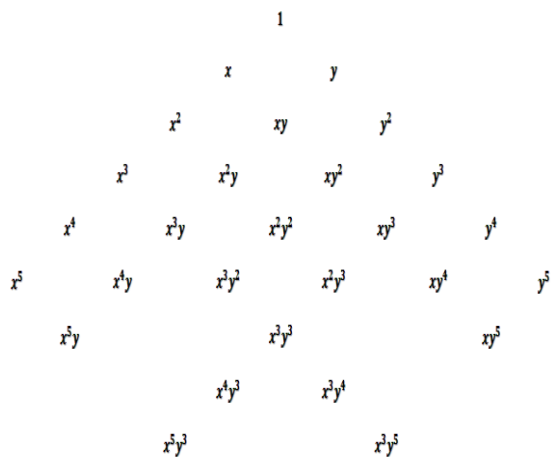
Figure 3. Polynomial terms contained in the Lagrange deflection expression for BWRE24.
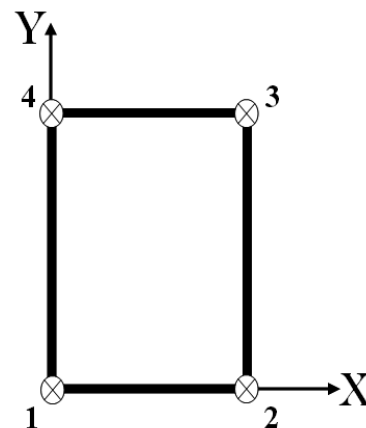
Figure 4. one rectangular element of BWRE24 .

As usual, the deflection function (14) can be formulated as,

$$w(x,y) = \lfloor H_w \rfloor \{\alpha\} \tag{15}$$

where,

$$\lfloor H_w \rfloor = \begin{bmatrix} 1 & x & y & x^2 & xy & \cdots & y^5(\frac{1}{2}xa - \frac{2}{3}x^3/a) \end{bmatrix} \text{ and } \{\alpha\} = \begin{Bmatrix} \alpha_1 \\ \alpha_2 \\ \vdots \\ \alpha_{24} \end{Bmatrix}$$

For one element, the 6 degrees of freedom at each node *i* can be written as:

$$\{w\}_i = \begin{Bmatrix} w \\ \phi_x \\ \phi_y \\ \epsilon_x \\ \epsilon_y \\ \epsilon_{xy} \end{Bmatrix} = \begin{vmatrix} H_w \\ H_{w,x} + h_0^2 \left(H_{w,xxx} + H_{w,xyy} \right) \\ H_{w,y} + h_0^2 \left(H_{w,yyy} + H_{w,yxx} \right) \\ H_{w,xx} + h_0^2 \left(H_{w,xxxx} + H_{w,xxyy} \right) \\ H_{w,yy} + h_0^2 \left(H_{w,yyyy} + H_{w,xxyy} \right) \\ 2H_{w,xy} + 2h_0^2 \left(H_{w,xyyy} + H_{w,xxxy} \right) \end{vmatrix} \{\alpha\} \tag{16}$$

By substituting with the local coordinates of the nodes: (0, 0), (a, 0), (a, b), (0, b) in the elements of $\lfloor H_w \rfloor$, the displacement vector can be expressed as:

$$\{w\} = \lfloor T_b \rfloor \{\alpha\} \tag{17}$$

Now, the monomers $\{\alpha\}$ can be obtained by

$$\{\alpha\} = \lfloor T_b \rfloor^{-1} \{w\} \tag{18}$$

And therefore, the formulation of the deflection function (15) can be written as [10]

$$W(x,y) = \lfloor H_w \rfloor \lfloor T_b \rfloor^{-1} \{w\} \tag{19}$$

where, the shape functions of the plate bending element are given by

$$\lfloor N_w \rfloor = \lfloor H_w \rfloor \lfloor T_b \rfloor^{-1} \tag{20}$$

Although, the sufficient number of boundary conditions for Bergan - Wang approach is three. However, as shown in the results tables (1), (2), (3), (4) taking M_n (with the subscript n referring to the normal direction at the plate boundary) as a boundary condition or not in the case of hard and soft simply supported, does not affect the central deflection results of the plate. So, M_n will not be taken as a degree of freedom in the second finite element model.

3.2. The second finite element which will be denoted BWRE36
The displacement field is introduced at each node (i) as:

$$\{w\}_i^T = \{w|\phi_x|\phi_y|\epsilon_{xy}\}_i \tag{21}$$

By using the new expressions based on Bergan – Wang approach in (3), (11), (12), the result of 4-degrees of freedom with the nine nodes is a rectangular finite element model of 36 degrees of freedom per element.

This element assures a complete polynomial of degree five:

$$
\begin{aligned}
w(x, y) = {} & \alpha_1 + \alpha_2 x + \alpha_3 y + \alpha_4 x^2 + \alpha_5 xy + \alpha_6 y^2 + \alpha_7 x^3 + \alpha_8 x^2 y + \alpha_9 xy^2 \\
& + \alpha_{10} y^3 + \alpha_{11} x^4 + \alpha_{12} x^3 y + \alpha_{13} x^2 y^2 + \alpha_{14} xy^3 + \alpha_{15} y^4 + \alpha_{16} x^5 \\
& + \alpha_{17} x^4 y + \alpha_{18} x^3 y^2 + \alpha_{19} x^2 y^3 + \alpha_{20} xy^4 + \alpha_{21} y^5 + \alpha_{22} x^5 y \\
& + \alpha_{23} x^4 y^2 + \alpha_{24} x^3 y^3 + \alpha_{25} x^2 y^4 + \alpha_{26} xy^5 \\
& + \alpha_{27} x^5 y^2 + \alpha_{28} x^4 y^3 + \alpha_{29} x^3 y^4 + \alpha_{30} x^2 y^5 + \alpha_{31} x^5 y^3 + \alpha_{32} x^4 y^4 \\
& + \alpha_{33} x^3 y^5 + \alpha_{34} x^5 y^4 + \alpha_{35} x^4 y^5 + \alpha_{36} x^5 y^5
\end{aligned}
\tag{22}
$$
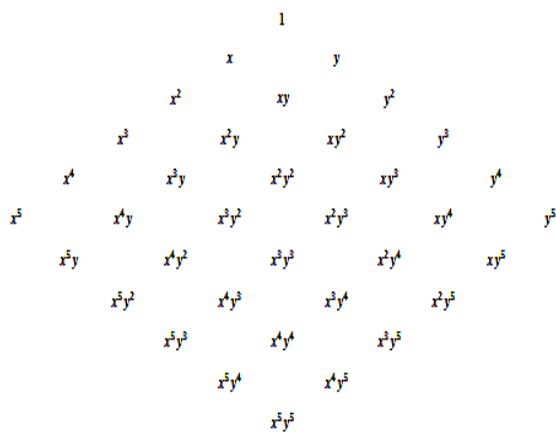
Figure 5. Polynomial terms contained in the Lagrange deflection expression for BWRE36.
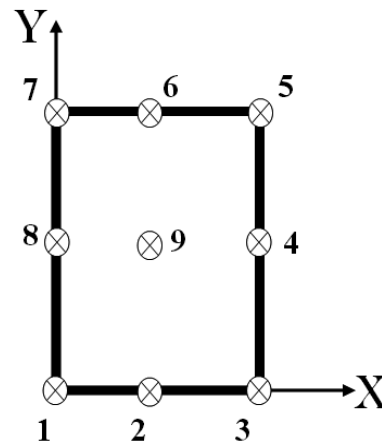
Figure 6. one rectangular element of BWRE36.

In general, the deflection function (22) can be formulated as (15),

$$
\lfloor H_w \rfloor = \lfloor 1 \quad x \quad y \quad x^2 \quad xy \quad y^2 \quad \cdots \quad x^5 y^5 \rfloor \text{ , and } \{\alpha\} = \begin{Bmatrix} \alpha_1 \\ \alpha_2 \\ \vdots \\ \alpha_{36} \end{Bmatrix}
$$

For one element, 4 degrees of freedom at each node i can be written as:

$$
\{w\}_i = \begin{Bmatrix} w \\ \phi_x \\ \phi_y \\ \epsilon_{xy} \end{Bmatrix} = \begin{bmatrix} H_w \\ H_{w,x} + h_0^2 \left(H_{w,xxx} + H_{w,xyy} \right) \\ H_{w,y} + h_0^2 \left(H_{w,yyy} + H_{w,yxx} \right) \\ 2H_{w,xy} + 2h_0^2 \left(H_{w,xyyy} + H_{w,xxxy} \right) \end{bmatrix} \{\alpha\}
\tag{23}
$$

By substituting with the local coordinates of each node (0, 0), (a/2, 0), (a, 0), (a, b/2), (a, b), (a/2, b), (0, b), (0, b/2), (a/2, b/2) in the elements of $\lfloor H_w \rfloor$, the displacement vector can be expressed as (17). And therefore, the monomers $\{\alpha\}$ and the shape functions of the plate bending element are given by (18) and (20) respectively.

4. Variation formulation of the stiffness matrix and load vector
By substituting the displacement field (11) and the strains (12) into the statement of the principle of virtual work to make the complementary energy $\Pi_b + \Pi_s - \Pi_{ext}$ (which is the difference of the strain

energy $\Pi_b + \Pi_s$ and of the work Π_{ext} which the surface stresses acts over that portion of the surface where the displacements are prescribed) is a minimum as [11]

$$0 = \int_{v_e} \left(\delta\epsilon_{xx}\, \sigma_{xx} + \delta\epsilon_{yy}\, \sigma_{yy} + 2\delta\epsilon_{xy}\, \sigma_{xy} + 2\delta\epsilon_{xz}\, \sigma_{xz} + 2\delta\epsilon_{yz}\, \sigma_{yz} \right) dv$$
$$+ \int_{\Omega_e} (\delta w\, q\, dx\, dy) - \oint_{\Gamma_e} (\delta\phi_n\, M_{nn} + \delta\phi_s\, M_{ss} + \delta w\, Q_n)\, ds \tag{24}$$

By using (12) the bending and shear strain energy and the external potential energy Π_b, Π_s and Π_{ext}, respectively can be written as,

$$\Pi_b = \int_{\Omega_e} \{\epsilon_b\}^T [D_b] \{\epsilon_b\}\, dA \tag{25-a}$$

$$\Pi_s = \int_{\Omega_e} \{\epsilon_s\}^T [D_s] \{\epsilon_s\}\, dA \tag{25-b}$$

$$\Pi_{ext} = \int_{\Omega_e} (\delta w\, q\, dx\, dy) - \oint_{\Gamma_e} (\delta\phi_n\, M_{nn} + \delta\phi_s\, M_{ss} + \delta w\, Q_n)\, ds \tag{25-c}$$

By substituting equations (20) and (16) into (12) in the first model BWRE24, and by equations (20) and (23) into (12) in the second model BWRE36, to formulate the bending strain vector $\{B_b\}$ and the shear strain vector $\{B_s\}$, and therefore, the element stiffness matrix can be written as [12]

$$[k^e] = [k_b^e] + [k_s^e] \tag{26}$$

where,

$$[k_b^e] = \iint_{A_e} \{B_b\}^T [D_b] \{B_b\}\, dA \tag{27}$$

$$[k_s^e] = \iint_{A_e} \{B_s\}^T [D_s] \{B_s\}\, dA \tag{28}$$

And by using the shape functions for each model $\{N_i\}$, the equivalent load vector can be obtained by

$$\{F^e\} = \iint_{A_e} \{N_i\}^T q\, dA \tag{29}$$

5. Numerical examples

In order to test the performance of the two finite element models BWRE24 and BWRE36, a square plate of side length $a = 1\, m$ subjected to uniform and concentrated load with different boundary conditions have been studied. The material properties of the plate are: Young's modulus E=71 GPa; Poisson's ratio $v = 0\cdot3$

For the uniform loading q the normalized central deflection is given by $\overline{w} = \frac{100*(w_c.Eh^3)}{12*(1-v^2)*q*a^4}$, and for the concentrated central loading P the normalized central deflection is given by $\overline{w} = \frac{100*(w_c.Eh^3)}{12*(1-v^2)*P*a^2}$ results are given for different thickness to span ratio $\frac{h}{a}$.

5.1. Case 1 simply supported at all edges of the plate.

5.1.1. Hard simply supported (BWRE24). Calculations have been done firstly by imposing 3 boundary conditions ($w = \phi_s = M_n = 0$) as it is specified by Mindlin-Reissner theory, and by imposing only 2 boundary conditions ($w = \phi_s = 0$) as used in the majority of existing finite element codes. Tables 1, 2, 3 and 4 give the obtained results with the mesh shown in (Fig.7).

Table 1. The normalized central deflection for hardly simply supported edge with boundary conditions (w = ϕ_s = M_n = 0)

h/a	0.001	0.01	0.05	0.1	0.15	0.2	0.25
Uniform load							
R-M *theory* [13]	0.4062	0.4062	0.4107	0.4273	0.4536	0.4906	0.5379
3D FEM [14]	-	-	-	0.4273	0.4536	0.5217	0.5656
BWRE24 (32x32)	0.4062	0.4062	0.4547	0.4703	0.4891	0.5322	0.6011
Central load							
R-M *theory* [15]	0.12441	0.12491	0.1343	0.15754	0.19283	0.24026	0.29983
BWRE24 (32x32)	0.11599	0.11855	0.1343	0.15567	0.18964	0.24303	0.31748

Thin Plate theory [16]:0.406 for uniform load and 0.1160 for central load

Table 2. The normalized central deflection for hardly simply supported edge with boundary conditions   (w = ϕ_s = 0)

| h/a	0.001	0.01	0.05	0.1	0.15	0.2	0.25
Uniform load							
BWRE24 (32x32)	0.4062	0.4062	0.4547	0.4703	0.4891	0.5322	0.6012
Central load							
BWRE24 (32x32)	0.11599	0.11855	0.1343	0.15565	0.18961	0.24300	0.3175

5.1.2. Soft simply supported (BWRE24). As has been done with hard simply supported, two situations have been considered: The first one when 3 boundary conditions (w = M_n = M_{ns} = 0) are imposed as it is specified by Mindlin-Reissner theory and in the second one, M_n is not specified and only 2 boundary conditions are imposed(w = M_{ns} = 0) .

Table 3. The normalized central deflection for softly simply supported edge with boundary conditions (w = M_n = M_{ns} = 0)

h/a	0.001	0.01	0.05	0.1	0.15	0.2	0.25
Uniform load							
R-M theory [17]	0.4065	0.4099	-	0.4616	-	-	-
BWRE24 (32x32)	0.4041	0.4045	0.4182	0.4384	0.4819	0.5483	0.6364
Central load							
BWRE24 (32x32)	0.11555	0.11689	0.1262	0.14863	0.18858	0.24702	0.32532

Table 4. The normalized central deflection for softly simply supported edge with boundary conditions (w = M_{ns} = 0)

h/a	0.001	0.01	0.05	0.1	0.15	0.2	0.25
Uniform load							
BWRE24 (32x32)	0.4041	0.4044	0.4181	0.4379	0.4809	0.5479	0.6381
Central load							
BWRE24 (32x32)	0.11555	0.11687	0.1261	0.14852	0.18836	0.24669	0.32569
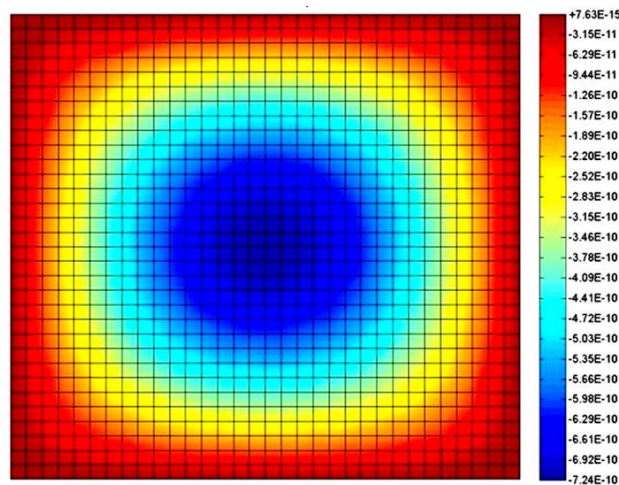
Figure 7. Deflection of each node on a square simply supported plate
discretized by 32x32 (BWRE24) FEM

It is clear that the imposition of the boundary condition $M_n = 0$ does not affect the results of central deflection. Moreover, the results emphasis the fact that as thickness becomes thin the values of the deflection coincide with classical plate theory results :(0.406 for uniform load and 0.1160 for central Load [16]).

On the other hand, as thickness increases, differences between results based on Bergan-Wang and those based on Reissner-Mindlin increases. This can be explained by the fact that Bergan-Wang approach is based on the assumption that the plate is moderately thick. Practically speaking, for: $\frac{h}{a} > 0.125$ the structure should be treated as 3D structures not a 2D one.

5.1.3. Hard simply supported (BWRE36). Calculations have been done by imposing only 2 boundary conditions $(w = \phi_s = 0)$ as used in the majority of existing finite element codes. Tables 5 and 6 give the obtained results with the mesh shown in (Fig. 8)

Table 5. The normalized central deflection for hardly simply supported edge with
boundary conditions $(w = \phi_s = 0)$

h/a	0.001	0.01	0.05	0.1	0.15	0.2	0.25
Uniform load							
R-M *theory* [13]	0.4062	0.4062	0.4107	0.4273	0.4536	0.4906	0.5379
3D FEM [14]	-	-	-	0.4273	0.4536	0.4906	0.5379
BWRE36 (16x16)	0.4062	0.4068	0.4301	0.4471	0.4738	0.5123	0.5691
Central load							
R-M *theory* [15]	0.12441	0.12491	0.1343	0.15754	0.19283	0.24026	0.29983
BWRE36 (16x16)	0.11600	0.11688	0.1265	0.14362	0.17155	0.20976	0.26385

Thin Plate theory [16]:0.406 for uniform load and 0.1160 for central load

5.1.4. Soft simply supported (BWRE36). Calculations have been done by imposing only 2 boundary conditions (w = M_{ns} = 0)

Table 6. The normalized central deflection for softly simply supported edge with boundary conditions ($w = M_{ns} = 0$)

h/a	0.001	0.01	0.05	0.1	0.15	0.2	0.25
Uniform load							
R-M *theory* [17]	0.4065	0.4099	-	0.4616	-	-	-
BWRE36 (16x16)	0.4030	0.4032	0.3915	0.4150	0.4579	0.5126	0.5800
Central load							
BWRE36 (16x16)	0.11532	0.11570	0.1179	0.13606	0.16735	0.21009	0.26440
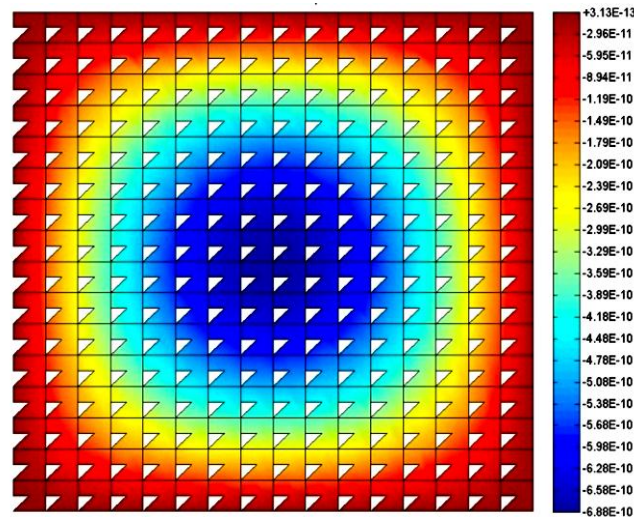
Figure 8. Deflection of each node on a square simply supported plate discretized by 16x16 elements by (BWRE36) FEM

5.2. Case 2 clamped at all edges of the plate.

5.2.1. Hard clamped (BWRE24 and BWRE36)

Table 7. The normalized central deflection for Hard clamped (w= ϕ_s = ϕ_n=0);

h/a	0.001	0.01	0.05	0.1	0.15	0.2	0.25
Uniform load							
R-M *theory* [13]	0.1265	0.1265	0.1327	0.1499	0.1787	0.2167	0.2675
3D FEM [14]	-	-	0.1325	0.1496	-	0.2135	0.2580
BWRE36 (16x16)	0.1265	0.1271	0.1349	0.1515	0.1781	0.2151	0.2659
BWRE24 (32x32)	0.1265	0.1280	0.1397	0.1615	0.1970	0.2485	0.3199
Central load							
R-M *theory* [15]	0.05855	0.05882	0.0652	0.08493	0.11732	0.16235	0.2197
BWRE36 (16x16)	0.05612	0.05656	0.0631	0.08013	0.10807	0.14668	0.1991
BWRE24 (32x32)	0.05610	0.05697	0.0663	0.08921	0.12707	0.18225	0.2572

Thin Plate theory [16]: 0.1265 for uniform load and 0.05612 for central load

5.2.2. Soft clamped (BWRE24 and BWRE36)

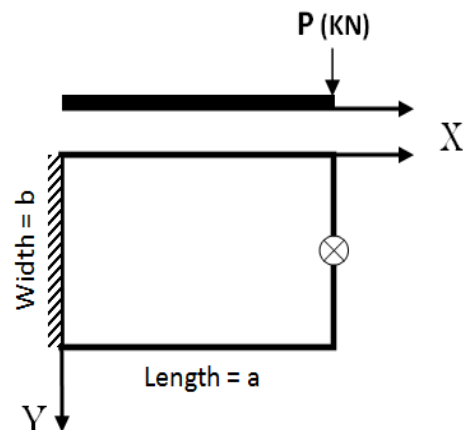**Table 8.** The normalized central deflection for soft clamped (w= $M_{ns} = \phi_n = 0$);

h/a	0.001	0.01	0.05	0.1	0.15	0.2	0.25
Uniform load							
BWRE36 (16x16)	0.1265	0.1271	0.1350	0.1533	0.1825	0.2227	0.2798
BWRE24 (32x32)	0.1265	0.1280	0.1400	0.1626	0.1988	0.2528	0.3271
Central load							
BWRE36 (16x16)	0.05611	0.05655	0.0632	0.08058	0.10922	0.14921	0.20238
BWRE24 (32x32)	0.05610	0.05696	0.0666	0.09007	0.12868	0.18481	0.26059

5.3. Case 3 cantilever plate.

The normalized deflection at the midpoint of the free side x=a of a cantilever (CFFF) Square plate is computed with BWRE36 and BWRE24 elements for different ratios of thickness / length of the plate (h/a) and is subjected to uniform load (Fig.9) and central load (Fig. 10) by imposing 3 boundary conditions on the clamped side as it is specified by Mindlin - Reissner theory and no boundary conditions on the other free sides
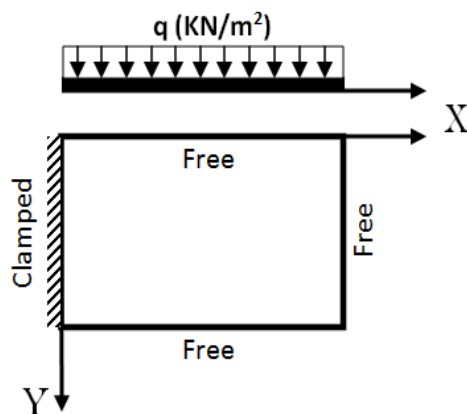
Figure 9. Cantilever plate subjects to uniform load	**Figure 10.** Cantilever plate subjects to concentrated load.

5.3.1. Hard clamped side and the others free

Table 9. The normalized deflection at the midpoint of the free side ($x = a$)
for a hard-clamped side ($w = \phi_s = \phi_n = 0$);

h/a	0.001	0.01	0.05	0.1	0.15	0.2
Uniform load						
R-M theory [18]	-	0.1278	-	0.1315	-	0.1375
BWRE36 (16x16)	0.12910	0.12915	0.1297	0.13088	0.13274	0.13301
BWRE24 (32x32)	0.12909	0.12918	0.1298	0.13125	0.13365	0.13719
Central load						
R-M theory [19]	-	0.36035	-	0.36684	-	0.38940
BWRE36 (16x16)	0.36156	0.36183	0.36474	0.36985	0.37787	0.38228
BWRE24 (32x32)	0.36154	0.36218	0.36608	0.37256	0.38335	0.39945

Thin Plate theory [16]: 0.12905 for uniform load and 0.36101 for central load

5.3.2. Soft clamped side and the others free

Table 10. The normalized deflection at the midpoint of the free side ($x = a$)
for a soft clamped side ($w = M_{ns} = \phi_n = 0$);

h/a	0.001	0.01	0.05	0.1	0.15	0.2
Uniform load						
BWRE36 (16x16)	0.12907	0.12912	0.12988	0.13164	0.13439	0.13672
BWRE24 (32x32)	0.12907	0.12915	0.13015	0.13233	0.13553	0.13994
Central load						
BWRE36 (16x16)	0.36152	0.36178	0.36515	0.37170	0.38212	0.39259
BWRE24 (32x32)	0.36152	0.36214	0.36695	0.37558	0.38874	0.40738

6. Conclusion

A new plate bending elements with a new degrees of freedom according to Bergan - Wang approach have been formulated as function of only the transversal deflection of the plate for the analysis of thin, moderately thick and thick rectangular plates with different types of boundary conditions, subjected to uniform and concentrated load, taking into account that they have a shape function of a complete polynomial of degree four and five.

When the plate thickness tends to the limit of thin plate, the element automatically has been converted to the classical plate theory, so that the shear locking is also avoided.

Numerical results show that Bergan-Wang approach can be easily implemented using the proposed elements leading to good results for relatively thick plates as well as very thin ones.

References

[1] Zhong, Y. and Q. Xu, 2017, Analysis bending solutions of clamped rectangular thick plate. *Mathematical Problems in Engineering*.

[2] Zienkiewicz, o. and Taylor, R. 2005, *The Finite Element Method Set ,6th Edition*. Butterworth-Heinemann.

[3] Hughes, A. C., 2012, The Finite Element Method: Linear Static and Dynamic Finite Element Analysis. Dover Civil and Mechanical Engineering.

[4] Abdalla, H. and K. Hassan, 1988, On the Bergan-Wang approach for moderately thick plates. *Communications in applied numerical methods*. 4(1): **p. 51-58**.

[5] Bergan, P.G. and X.Wang, 1984, Quadrilateral plate bending elements with shear deformations. *Computers & Structures*. 19(1-2): **p. 25-34**.

[6] Oñate, E., Structural analysis with the finite element method. Linear statics: volume 2: beams, plates and shells, 2013 Springer Science & Business Media.

[7] Ugural, A.C., *Stresses in plates and shells*, 1998, 2nd revised edition,McGraw-London.

[8] Jawad, M. , 2012, *Theory and design of plate and shell structures*. Springer Science & Business Media.

[9] Popplewell, N. and D. McDonald, 1971, Conforming rectangular and triangular plate-bending elements. *Journal of Sound and Vibration*, 19(3): **p. 333-347**.

[10] AboElsooud, M.T., 2003, Vibration control of plates using periodically distributed shunted piezoelectric patches. *University of Maryland, College Park*.

[11] Reddy, J.N., 1994*, An introduction to the finite element method*. Vol. 2, McGraw-Hill Boston.

[12] Soh, A.-K., et al., 2001, A new twelve DOF quadrilateral element for analysis of thick and thin plates. *European Journal of Mechanics-A/Solids*. 20(2): **p. 299-326**.

[13]   Ozkul, T.A. and U. Ture, 2004, The transition from thin plates to moderately thick plates by using finite element analysis and the shear locking problem. *Thin-Walled Structures*,. 42(10): **p. 1405-1430.**

[14]   Yudan Gou; Yongchang Cai; Hehua Zhu, 2018 A Simple High-Order Shear Deformation Triangular Plate Element with Incompatible Polynomial Approximation, *Tongji University Press*: Shanghai 200092, China.

[15]   Fuh-Gwo, Y. and R.E. Miller, 1988, A rectangular finite element for moderately thick flat plates. *Computers & structures*. 30(6): **p. 1375-1387**.

[16]   Timoshenko, S.P. and S. Woinowsky-Krieger, 1959, *Theory of plates and shells*. McGraw-hill.

[17]   J. Jirousek, Wroblewski, A Szybiński, B., 1995, A new 12 DOF quadrilateral element for analysis of thick and thin plates. *International journal for numerical methods in engineering*, Vol. 38: **p. 2619-2638**.

[18]   Xiao, Y., N. Jian-guo, and C. Chang-jun, 1992, Bending of cantilever rectangular plates with the effect of transeverse shear deformation. *Applied Mathematics and Mechanics*. 13(1): **p. 61-75**.

[19]   Peng-cheng, Lin, 1982, Bending of cantilever rectangular plate with concentrated load. *Applied Mathematics and Mechanics*. 3(2): **p. 281-291**.